

## ANALYSES OF PLANE STRESS DISCONTINUITY LINES SYSTEMS IN OYANE POROUS MEDIA

W. B o d a s z e w s k i

Kielce University of Technology

Tysiąclecia P.P. 7, 24-314 Poland

e-mail: wboda@tu.kielce.pl

The paper presents the results of numerical analyses of certain properties of plane stress discontinuity lines systems, which are specific for the Oyane condition, and do not appear when one assumes other yield conditions, such as Huber-Mises or Tresca conditions.

The results have been obtained by applying general algorithms that do not require formulating any individual relationships. The algorithms aid solving problems for any boundary conditions, of practically any type, which can be met in the problems of construction of discontinuous statically admissible fields, mainly the limit fields. In the assumed formulation, the solution consists in finding initially the fields arising around isolated nodes of stress discontinuity lines, and then integrating the fields into two-dimensional complex fields.

Application of these algorithms makes it possible to quickly find all the existing solutions of the stress discontinuity lines around the nodes, at the same time eliminating the need of forecasting (guessing the solution), which until recently was the main difficulty in solving each new complex field.

Physical justification of the Oyane condition is beyond the scope of this work.

**Key words:** shape design, limit analysis, numerical methods.

### NOTATIONS

$\alpha, \beta$	indexes of homogeneous stress state regions on physical plane,
$\{a\}$	global plane system,
$\{\xi\}^{(\alpha)}$	local plane system associated with principal stress directions in homogeneous region $\alpha$ ,
$\sigma_{pl}$	yield point of material without pores (material of skeleton),
$f_v$	porosity ratio ( $f_v = \frac{V_v}{V_v + V_s}$ , where: $V_v$ is the volume of voids, and $V_s$ the volume of skeleton of isotropic porous material),
$\mathcal{L}$	stress discontinuity line,
$\mathcal{L}^{\alpha, \beta}$	line separating adjacent regions $\alpha$ and $\beta$ ,
$\sigma$	stress tensor,
$\sigma_{ij}^{(\alpha)}$	stress tensor components in homogeneous region $\alpha$ ( $i, j = 1, 2$ ),
$\sigma_i^{(\alpha)}$	principal stresses in homogeneous region $\alpha$ ( $i = 1, 2$ ),
$\mathbf{p}$	stress vector,
$\omega$	stress parameter ( $\omega \in [0, 360]$ or $\in \omega [0, 180]$ ),
$\omega^{(\alpha)}$	stress parameter $\omega$ in homogeneous region $\alpha$ ,

$\{\overset{(\alpha)}{\omega}, \overset{(\beta)}{\omega}\}$	parametric spaces,
$\overset{(\alpha)}{x}$	stress multiplier in homogeneous region $\alpha$ ( $x \in [0,1]$ ),
$\overset{(\alpha)}{\phi}$	angle of principal stresses in homogeneous region $\alpha$ , defined in system $\{a\}$ ; it is the angle that the $a_1$ axis makes with the direction of the larger principal stress component,
$e^{\alpha,\beta}$	unit vector normal to line $\mathcal{L}^{\alpha,\beta}$ directed towards outside of region $\alpha$ ( $e^{\alpha,\beta} = -e^{\beta,\alpha}$ ),
$\nu^{\alpha,\beta}$	angle determined for direction of $e^{\alpha,\beta}$ , defined in system $\{a\}$ ,
$Q^{\alpha,\beta} = 1,2; q^{\alpha,\beta} = 1,2,3,4$	families and subfamilies of stress discontinuity line $\mathcal{L}^{\alpha,\beta}$ , $q^{\alpha,\beta} = 1,3$ are assigned to $Q^{\alpha,\beta} = 1$ , and $q^{\alpha,\beta} = 2,4$ are assigned to $Q^{\alpha,\beta} = 2$ ,
$\Delta\gamma = \Delta\gamma(\overset{(\alpha)}{\omega}, \overset{(\beta)}{\omega}, q^{\alpha,\beta})$	function expressing the angular parameter that determines versor $e^{\alpha,\beta}$ , defined in local system $\{\xi\}^{(\alpha)}$ ( $\Delta\gamma \in [0, 2\pi]$ ), $\beta$ region adjacent to $\alpha$ ,
$\Delta\phi = \Delta\phi(\overset{(\alpha)}{\omega}, \overset{(\beta)}{\omega}, Q^{\alpha,\beta}) \equiv \overset{(\beta)}{\phi} - \overset{(\alpha)}{\phi}$	function expressing differences between the angles of principal stresses in adjacent homogeneous regions $\alpha$ and $\beta$ , defined in local system $\{\xi\}^{(\alpha)}$ ( $\Delta\phi \in [-\frac{\pi}{2}, \frac{\pi}{2}]$ ),
$\Delta\nu^{(\alpha)} \equiv \nu^{\alpha,\alpha+1} - \nu^{\alpha-1,\alpha}$	angle between lines $\mathcal{L}^{\alpha-1,\alpha}$ and $\mathcal{L}^{\alpha,\alpha+1}$ ,
$\Lambda$	region of existence line $\mathcal{L}$ ;
$\Lambda_{1,N}^{\alpha,\alpha+1}$	admissible subregion of variability $\overset{(\alpha)}{\omega}, \overset{(\alpha+1)}{\omega}$ obtained for the settled values: $\overset{(1)}{\omega}, \overset{(N)}{\omega}, N$ ,
$\Gamma$	interval of existence line $\mathcal{L}$ ,
$\Gamma_{1,N}^{(\alpha)}$	admissible interval of variability $\overset{(\alpha)}{\omega}$ obtained for the settled values: $\overset{(1)}{\omega}, \overset{(N)}{\omega}, N$ ,
$\delta$	angle between outer stress discontinuity lines of field around node,
$N$	number of homogeneous regions in field around node.

## 1. INTRODUCTION

### 1.1. Introductory remarks

We will consider plane, statically admissible, discontinuous stress fields, which are piecewise homogeneous, and whose stress discontinuity lines  $\mathcal{L}$  are segments of straight lines. Application of such fields is based on the lower bound theorem which is known from the limit analysis. The fields can be applied to finding a lower bound of the limit load causing plastic yielding of structure elements of a given shape, or for approximate shaping of these elements (W. SZCZEPIŃSKI, [1]).

In both formulations, only the boundary conditions are given, and one needs to find the statically admissible stress field, inscribed within the boundaries,

which in each point fulfils the assumed yield condition, or at least guarantees that this condition is not exceeded. These formulations are characteristic for the method known under the already well-recognised acronym of SADSF.

It is worth noticing at the very beginning that the set of unknowns in such problems consists not only of stress components in the homogeneous regions and the co-ordinates of the line nodes, but it also includes the system of stress discontinuity lines itself – as this system is not given *a priori*. If one assumes it arbitrarily, then for the given boundary conditions the solution might not exist, and in most cases it does not exist. The solution exists only for some particular line systems, depending on the boundary conditions; however, one cannot find any formulae, which would express this dependence ([8, 9]). In other words, at the start point, even the system of conditions, which one should formulate for solving the boundary problem, remains unknown.

The mentioned fact explains the greatest difficulty that appears in any problem concerning construction of stress discontinuity line systems. It explains why, among other things, these systems have been solved, for many decades, by postulating and verifying the solution, and the attempts of formulating the problem in an algorithmic form have failed for such a long time.

The author was encouraged to undertake the analysis of stress discontinuity line systems in porous media by the results reported in works [4, 5]. In these works, the line systems were assumed *a priori* on the basis of already-known solutions, but those had been obtained for the Huber–Mises yield condition.

The aim of the work was to examine the specificity of properties of the system of discontinuity lines, which appear for the Oyane condition in a plane stress, and which do not appear in the case of the Huber–Mises and Tresca conditions. The results presented here have been obtained during testing general algorithms for the analysis of stress discontinuity line systems [9], while the Oyane condition was substituted to these algorithms.

These are the algorithms, in which discontinuous statically admissible stress fields are treated as certain abstract objects, which are described exclusively by the systems of conditions that define such fields. For this reason, the objects have only those properties that result from the mentioned conditions. Introducing any further-going assumptions usually leads to wrong results, for example it may cause that some roots of the solutions are lost.

### 1.2. Outline of the investigation method

The equilibrium equations formulated for each line  $\mathcal{L}^{\alpha,\beta}$  separating homogeneous states of stress  $\sigma^{(\alpha)}$ ,  $\sigma^{(\beta)}$  in adjacent regions  $\alpha$  and  $\beta$  of the statically admissible field have the form (see Fig. 1 [8, 9])

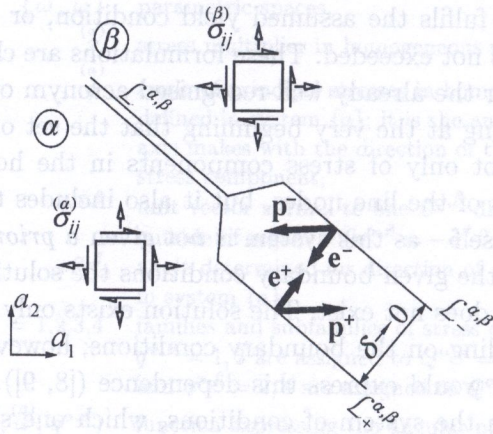


FIG. 1.

$$(1.1) \quad \left( \sigma_{ij}^{(\alpha)} - \sigma_{ij}^{(\beta)} \right) e_i = 0 \quad \left( i, j = 1, 2; \alpha \neq \beta; \sigma^{(\alpha)} \neq \sigma^{(\beta)} \right),$$

where  $e$  is a unit vector normal to  $\mathcal{L}^{\alpha, \beta}$ . One can see that the system is homogeneous, so that non-zero solutions exist if

$$(1.2) \quad \det \left| \sigma_{ij}^{(\alpha)} - \sigma_{ij}^{(\beta)} \right| = 0.$$

The other set of conditions is the content of solutions  $e_i$  in the domain  $(0 \leq (e_i)^2 \leq 1)$ , which – when considering (1.2) – leads to two conditions:

$$(1.3) \quad 0 \leq \frac{\sigma_{AA}^{(\alpha)} - \sigma_{AA}^{(\beta)}}{\sigma_{jj}^{(\alpha)} - \sigma_{jj}^{(\beta)}} \leq 1, \quad \left( \sigma^{(\alpha)} \neq \sigma^{(\beta)} \right) \\ (\alpha \neq \beta; \quad j, A = 1, 2; \quad A - \text{is not summed})$$

set for  $A = 1$  and  $A = 2$ .

Condition (1.2) is called the equality condition of existence of line  $\mathcal{L}^{\alpha, \beta}$ , while conditions (1.3) are known as the inequality conditions determining the domain of solutions of the system (1.1). In the limit fields, the yield condition is also added, while in non-limiting ones the inequality condition is applied.

It can be noticed that among the above-mentioned conditions, none is determined on the parameters determining either the number of lines  $\mathcal{L}^{\alpha, \beta}$ , or the structure of link system of these lines. In fact, we deal with the problem in which the system of conditions is not given beforehand.

In this situation, which apparently might seem hopeless, one could find a positive solution, anyway. Discontinuous stress field does not need to be treated as the field consisting of homogeneous regions separated by stress discontinuity lines. Its other universal components could also be the fields around nodes, and these can be solved by creating universal algorithms, as shown in work [9].

For the algorithms, the essential matter is to have at one's disposal the yield condition in a parameterized form. The aim of parameterization is not only to reduce the set of variables but, most of all, to create the possibility of constructing appropriate mapping and being able to generate beforehand the domains (1.3), what determines the efficiency of numerical procedures.

The Oyane yield condition [2, 4, 5] for plane stress state can be written in the form:

$$(1.4) \quad \eta(f_v)(\sigma_1 + \sigma_2)^2 + (\sigma_1 - \sigma_2)^2 = 4k^2\theta(f_v).$$

The functions of the porosity ratio:  $\theta(f_v)$ ,  $\eta(f_v)$  are defined as follows:

$$\theta = (1 - f_v)^4, \quad \alpha = \frac{1}{\left[1 + \frac{\sqrt{1 - f_v}}{f_v}\right]^2}, \quad \eta = \frac{1 + 4\alpha}{3},$$

while the constant  $k = \sigma_{pl}/\sqrt{3}$  is equal to the yield point of the skeleton material under pure shear.

Condition (1.5) will be satisfied identically if we express the stress components  $\sigma_1$ ,  $\sigma_2$  as functions of the parameter  $\omega$ :

$$(1.5) \quad \begin{aligned} \sigma_1 &= xk\sqrt{\theta(f_v)} \left[ \sqrt{\frac{1}{\eta(f_v)}} \cos \omega + \sin \omega \right] \\ \sigma_2 &= xk\sqrt{\theta(f_v)} \left[ \sqrt{\frac{1}{\eta(f_v)}} \cos \omega - \sin \omega \right] \end{aligned}$$

and substitute there  $x = 1$ .

In the formulae (1.5),  $\omega$  is a parameter from the interval  $[0, 180]^{1)}$  (the values from the remaining interval can be obtained by swapping the indices of principal stresses), and  $x$  is a multiplier from the interval  $[0, 1]$ , which allows us to take into account also non-limit states of stress.

The limit curve obtained for the condition (1.5) is shown in Fig. 2 (curve 1) along with the inscribed ellipse (curve 2), which is analogical to that obtained for

<sup>1)</sup>By convention, the values of  $\omega$  are expressed in degrees, and it is important when we use formulae (1.5), or convert degrees into radians. However,  $\omega$  is only a parameter, which generally has no meaning of an angle. For this reason, it is written as a number.

the Huber–Mises condition, but proportionally scaled down. Both curves were determined for a particular value of porosity ratio  $f_v$  equal to 0.29181982753, actually accepted in the investigation in order to facilitate inputting the data. At the same time, this value represents such a level of voids in the material, for which the porosity effect is well visible.

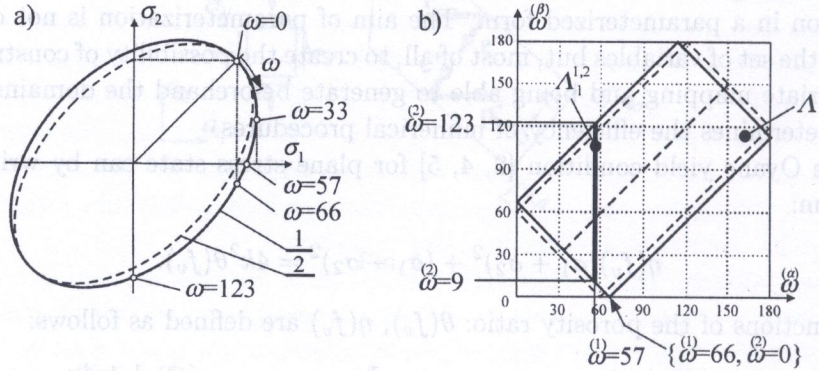


FIG. 2.

Next to this figure, the plots in Fig. 2b present graphical interpretation of the conditions of existence (1.3) obtained in the space  $\{\omega^{(\alpha)}, \omega^{(\beta)}\}$  when (1.5) is substituted into (1.3). This is the region of existence  $\Lambda$  determined in the mentioned space for the Oyane condition and for the assumed  $f_v$ .

As it can be seen, the region has a rectangular shape, as in the case of Huber–Mises condition, but this time, with Oyane condition, the size of the region is variable and depends on porosity ratio  $f_v$ . For  $f_v = 0$ , the region is identical with that for the Huber–Mises condition (broken line), but with increasing  $f_v$  one of the sides of the rectangle becomes shorter, while the other expands. For example, with the assumed value of  $f_v$ , the coordinate of the lower vertex shifts from  $\omega = 60$  for material without pores, to  $\omega = 66$  for the porous one.

In the following part, we will consider the fields around the nodes (Fig. 3), in which homogeneous regions  $\alpha$  are enumerated with consecutive natural numbers  $1..N$ , and whose states of stress are represented by  $\omega^{(\alpha)}, \phi^{(\alpha)}$  ( $\alpha = 1..N$ ), where  $\phi^{(\alpha)}$  is the angle of principal stresses in region  $\alpha$ . The parameter  $\omega^{(\beta)}$  from Fig. 2b will then have the meaning  $\omega^{(\alpha+1)}$ .

Substituting the parameterization equation (1.5) into the equilibrium equations, and taking into account the equality condition of existence (1.2), we obtain recursive formulae for the functions:

$$(1.6) \quad \Delta\phi = \Delta\phi\left(\omega^{(\alpha)}, \omega^{(\alpha+1)}, Q^{\alpha, \alpha+1}\right) \quad \Delta\gamma = \Delta\gamma\left(\omega^{(\alpha)}, \omega^{(\alpha+1)}, q^{\alpha, \alpha+1}\right).$$

Figure 3b illustrates the meaning of these functions. One can see that  $\Delta\phi$  is the angle of principal stresses in the region  $\alpha + 1$  measured with respect to the axis  $\xi_1$  of the system  $\{\xi\}^{(\alpha)}$  associated with the directions of principal stress in the preceding region  $\alpha$ . In turn,  $\Delta\gamma$  is the angular parameter of the unit vector  $\mathbf{e}$ , normal to line  $\mathcal{L}^{\alpha,\alpha+1}$ , and measured with respect to the same axis of the system  $\{\xi\}^{(\alpha)}$ .

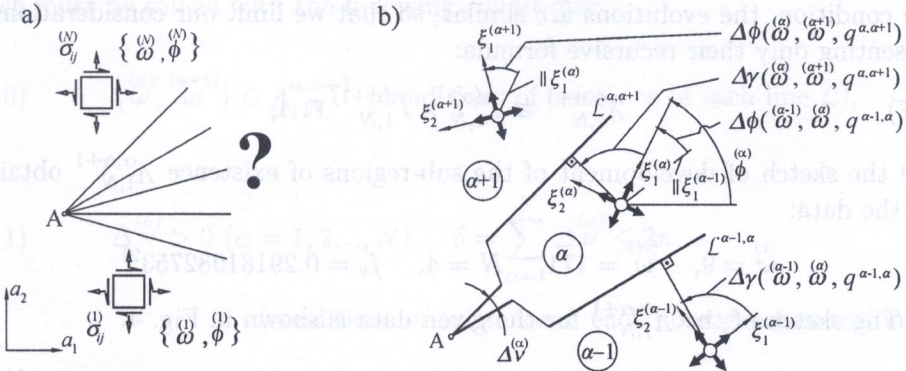


FIG. 3. a) Boundary conditions and graphical formulation of the problem for field around node; b) notations used in local systems  $\{\xi\}^{(\alpha)}$ .

We omit presenting functions (1.6) in explicit forms. The functions are very complicated and difficult to transform, so it is better to leave them in the form of the algorithms, and analyse them numerically.

In formulae (1.6), the parameters of line families  $\mathcal{L}^{\alpha,\alpha+1}$  are denoted with  $Q = 1, 2$ , while  $q = 1, 2, 3, 4$  pertains to their subfamilies. In fact, these are the indices of the roots. The values  $Q = 1$  and  $Q = 2$  refer to  $q = 1, 3$  and  $q = 2, 4$ , respectively.

In solving an arbitrary boundary problem that could be met in the fields around nodes, it is possible to single out four elementary problems ([9]). One of them, most extensively used in this work, is the following problem:

for the given states of stress in the outer regions 1 and  $N$  (Fig. 3a):

$$\{\omega^{(1)}, \phi^{(1)}, \omega^{(N)}, \phi^{(N)}\};$$

one should determine:

$$\{N, \omega^{(2)}, \dots, \omega^{(N-1)}, q^{1,2}, q^{2,3}, \dots, q^{N-1,N}\},$$

which means to find the number of regions of the field  $N$  and the states of stress in its internal regions, taking into account only the solutions that exist on the physical plane.

Obviously, it must be done in a numerical way. Then, the control over the content of variables in the domain becomes an essential task. Note that when the stress parameters are fixed in the outer regions  $\omega^{(1)}, \omega^{(N)}$ , then, simultaneously, additional constraints are imposed on the domains of parameters  $\omega^{(2)}, \dots, \omega^{(N-1)}$  in the internal regions. The evolutions of domains, pertaining to this situation, are described in detail in work [9] for the Huber–Mises condition. For the Oysane condition, the evolutions are similar, so that we limit our considerations to presenting only their recursive formula:

$$(1.7) \quad \Lambda_{1,N}^{\alpha,\alpha+1} \equiv \Gamma_{1,N}^{(\alpha)} \times \Gamma_{1,N}^{(\alpha+1)} \cap \Lambda,$$

and the sketch of development of the sub-regions of existence  $\Lambda_{1,N}^{\alpha,\alpha+1}$  obtained for the data:

$$\omega^{(1)} = 9, \quad \omega^{(N)} = 171, \quad N = 4, \quad f_v = 0.29181982753^2)$$

The sketch of the  $\Lambda_{1,N}^{\alpha,\alpha+1}$  for the given data is shown in Fig. 4.

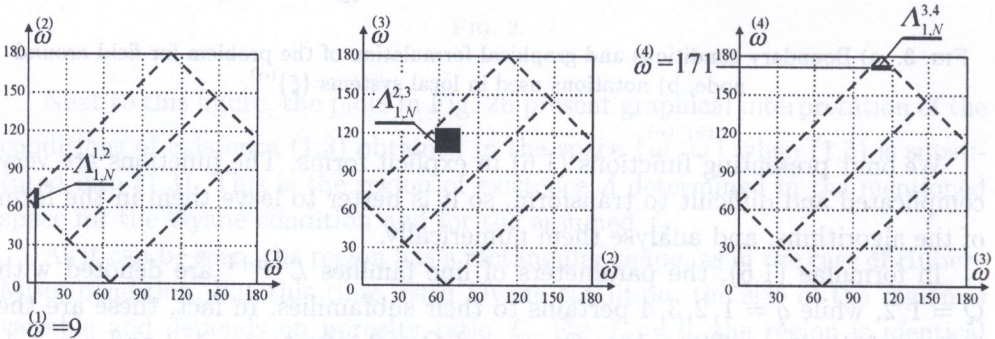


FIG. 4.

In other words, for the fixed  $\{\omega^{(1)}, \omega^{(N)}\}$ , the domains  $\Lambda_{1,N}^{\alpha,\alpha+1}$  of stress parameters for each couple of adjacent regions are determined beforehand, and next the following conditions are formulated:

$$\{\omega^{(\alpha)}, \omega^{(\alpha+1)}\} \in \Lambda_{1,N}^{\alpha,\alpha+1}.$$

According to Fig. 3b, one can also write the formula for the value of parameter:

$$(1.8) \quad \Delta\nu^{(\alpha)} \equiv \Delta\nu \left( \omega^{(\alpha-1)}, \omega^{(\alpha)}, \omega^{(\alpha+1)}, q^{\alpha-1,\alpha}, q^{\alpha,\alpha+1} \right),$$

which expresses the angle between two consecutive stress discontinuity lines.

<sup>2)</sup>For these data we obtained (see also Fig. 4):

$$\Gamma_{1,N}^{(1)} = [9.0, 9.0], \quad \Gamma_{1,N}^{(2)} = [57.0, 75.0], \quad \Gamma_{1,N}^{(3)} = [105.0, 123.0], \quad \Gamma_{1,N}^{(4)} = [171.0, 171.0].$$

Finally, single equation can be derived to solve the problem:

$$(1.9) \quad \phi^{(N)} - \phi^{(1)} = \sum_{\alpha=1}^{N-1} \Delta\phi \left( \omega^{(\alpha)}, \omega^{(\alpha+1)}, Q^{\alpha, \alpha+1} \right),$$

which must be solved with the following conditions:

$$(1.10) \quad \{ \omega^{(\alpha)}, \omega^{(\alpha+1)} \} \in \Lambda_{1,N}^{\alpha, \alpha+1} \quad (\text{conditions of existence of each line } \mathcal{L}),$$

$$(1.11) \quad \Delta\nu^{(\alpha)} > 0 \quad (\alpha = 1, 2, \dots, N), \quad \delta = \sum_{\alpha=1}^N \Delta\nu^{(\alpha)} \leq 2\pi$$

(conditions of existence of each homogeneous region  $\alpha$ )

and, possibly, with taking into account additional geometrical limitations.

In software implementation of the problem, the solutions are depicted as graphs of the fields on a physical plane ([9]). All existing solutions are presented there.

In order to construct a complex field from them, it suffices to choose the ones which create a net to secure a physical place for the realisation of the particular stress states.

### 1.3. Purpose of investigation

In the undertaken investigations, the author considered the cases characteristic for the systems of lines appearing when assuming the Oyane condition and plane stress. The essential aim of the investigation was finding the answers to the following questions:

- What are the significant differences between typical, known systems of stress discontinuity lines obtained for the Huber–Mises condition, and those for the Oyane condition.
- How to construct the systems of stress discontinuity lines in Oyane-type limit fields in such a way that one could make use of already known structures of such line systems found for the Huber–Mises, or possibly also Tresca conditions.

Physical justification of the Oyane condition is exhaustively presented in papers [4, 5]; in this work this problem will not be considered.

## 2. RESULTS OF ANALYSES

2.1. *The essence of distinctness of stress discontinuity line systems in Oyane fields*

In the analyses, as well as in the software implementation used in the investigation, a specific value of porosity ratio  $f_v$  was assumed, as mentioned in the previous section. The limit curve, determined for that value and the Oyane condition, is shown in Fig. 2a (curve 1). As it can be seen, the curve is not an ellipse, which becomes evident when we compare the limit curve with an inscribed actual ellipse (curve 2) in Fig. 2.

To avoid introducing special definitions of characteristic points on the Oyane curve, we will continue describing it by means of the parameter  $\omega$  and the numerical values. For the assumed value of  $f_v$  we have (see Fig. 2a,b):

- The state of biaxial isotropic tension when  $\omega = 0$ ; the values of principal stresses are then  $\sigma_1(0) = \sigma_2(0) = 0.44587 \cdot \sigma_{pl}$ , where  $\sigma_{pl}$  is the yield point of material without pores, i.e. for  $f_v = 0$ .
- The state of uniaxial tension for  $\omega = 57$ , while  $\sigma_1(57) = 0.48568 \cdot \sigma_{pl}$ .
- The state of uniaxial compression for  $\omega = 123$ ; in this case:  $\sigma_2(123) = -0.48568 \cdot \sigma_{pl}$ .
- Maximum normal stress obtained for  $\omega = 33$ , while  $\sigma(33) = 0.5316406 \cdot \sigma_{pl}$ .

In non-limited fields, constructed in further part of the example, we will also use the quotient:  $x = \sigma_1(0)/\sigma_1(57) = 0.44587/0.48568$ , whose value equals 0.91803923.

Analysing these characteristic points on the Oyane curve we notice that the stresses  $\sigma_1(0) = \sigma_2(0) = 0.44587 \cdot \sigma_{pl}$  pertaining to the state of biaxial isotropic tension are lower than those obtained for the state of uniaxial tension, which are equal to  $\sigma_1(57) = 0.48568 \cdot \sigma_{pl}$ . It can be deduced from the graph of Oyane limit curve (Fig. 2a), where appropriate lines are drawn, and also from the graph of region of existence  $\Lambda$  (Fig. 2b), which shows that the limit state adjacent to the assumed  $\overset{(2)}{\omega} = 0$  can only be the limit state pertaining to  $\overset{(1)}{\omega} = 66$ . We can also realise that, for  $\overset{(1)}{\omega} = 57$ , the interval of parameters  $\overset{(2)}{\omega}$  in the adjacent region spreads over the values [9, 123], so that it does not include the point  $\overset{(2)}{\omega} = 0$ .

In effect, one of the most frequently used limit systems of stress discontinuity lines (Fig. 5), applied in the region of converging tension (or compression) strips ([1]) that is admissible, for example, for the Huber–Mises condition, in the case of Oyane condition is no longer an admissible system, or it is not a limit one. If we assume  $\sigma_1(57) = 0.48568 \cdot \sigma_{pl}$  in the strips, then in the region ABC the yield condition will be exceeded. However, when assuming that  $\sigma_1(0) = \sigma_2(0) = 0.44587 \cdot \sigma_{pl}$  in this region, the stresses in the strips must also be equal to  $\sigma_1 = 0.44587 \cdot \sigma_{pl}$ , and the limit state would not be reached there.

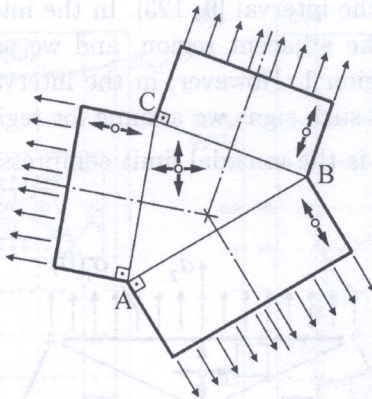


FIG. 5.

In the libraries of particular solutions used in the application version of the SADSF method and in its software implementations (for example [10]), the field from Fig. 5 is denoted with a two-character symbol  $z0$ , and this symbol will also be used in the present work.

Because the system of stress discontinuity lines of the field type  $z0$  is used in a vast majority of systems known for the Huber–Mises and Tresca conditions, the impact of the mentioned particular property of the Oyane condition is equally extensive. Then, we should either seek for entirely new solution, or try to preserve known systems of stress discontinuity lines and stresses, putting aside the question of achieving limit state in the strips of field  $z0$ , which means assuming there the stress multiplier  $x = 0.91803923$ , which leads to  $\sigma_1(57) = 0.44587 \cdot \sigma_{pl}$ .

If one seeks for new solutions specific for the Oyane condition, the obvious way is to examine first a system of stress discontinuity lines characteristic for a known field type  $d1$  (see Fig. 6, [1]) which, on its boundaries  $\{3,4\}$  and  $\{1,2\}$ , takes loads in the form of normal stresses of different values. In particular, it would be desirable to find such a limit field of type  $d1$  or other, which is loaded with stresses of values  $\sigma_1(57)$  on one boundary, and  $\sigma_1(0)$  on the other. Such solutions will be presented in the next section.

### 2.2. Obtained results

For the field type  $d1$ , we assume the state of uniaxial tension in homogeneous regions 2 and 4 (Fig. 6). We then have there  $\overset{(2)}{\omega} = \overset{(4)}{\omega} = 57$  and  $\overset{(2)}{\sigma}_1(57) = 0.48568 \cdot \sigma_{pl}$ . For the fixed value  $\overset{(2)}{\omega} = 57$ , we draw the conclusion, based on the region of existence  $\Lambda$  (Fig. 2b), that the parameter  $\omega$  in the adjacent regions

1 and 3 can vary within the interval [9, 123]. In the interval [9, 57) we have the same signs of stress in the adjacent region, and we assume the same interval of stress variability in region 1. However, in the interval (57, 123), the signs of stresses are different, and such signs we assume for region 3. With  $\omega = 123$ , the state adjacent to  $\omega^{(2)} = 57$  is the uniaxial limit compression.

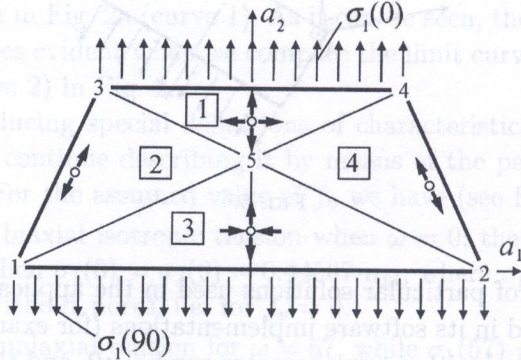


FIG. 6. Field parameters:  $\{(\overset{(1)}{\omega} = 0, \overset{(1)}{x} = 1), (\overset{(2)}{\omega} = \overset{(4)}{\omega} = 57, \overset{(2)}{x} = \overset{(4)}{x} = 0.91803923), (\overset{(3)}{\omega} = 90, \overset{(3)}{x} = 1)\}$ .

Then, in the presented investigations on the coupling of stress states in the field type  $d1$ , we have assumed that  $\overset{(1)}{\omega}$  takes values from the interval [9, 57), and  $\overset{(2)}{\omega} = 57$  is fixed. Consequently, we calculate the values  $\overset{(3)}{\omega}$  (numbers of the regions according to Fig. 6). The fields type  $d1$  are so easy to investigate that one actually needs to analyse only their internal node 5.

Two obvious cases were considered, when  $\overset{(1)}{\phi} = 0^\circ$ , and when  $\overset{(1)}{\phi} = 90^\circ$ , and the obtained results are presented as graphs shown in Figs. 7a and 7b.

As it can be seen, limit states can only be obtained in the whole field type  $d1$  if one takes the angle values from the intervals (approximately):  $\overset{(2)}{\phi} \in (70^\circ, 90^\circ)$  – for  $\overset{(1)}{\phi} = 90^\circ$  and  $\overset{(2)}{\phi} \in (0^\circ, 20^\circ)$  – for  $\overset{(1)}{\phi} = 0^\circ$ .

With  $\overset{(2)}{\phi} \in (20^\circ, 70^\circ)$ , the limit field can not be constructed for the assumed system of lines. Let us also notice that the stress  $\overset{(1)}{\sigma}_1$  in region 1 is always greater than that obtained for  $\omega = 57$ , which means that it is not possible to draw a strip loaded with the limit uniaxial tensile stress out of the top of the field. Then, this field is not suitable for creating branching of the strips, in contrast to the case of the field type  $z0$ .

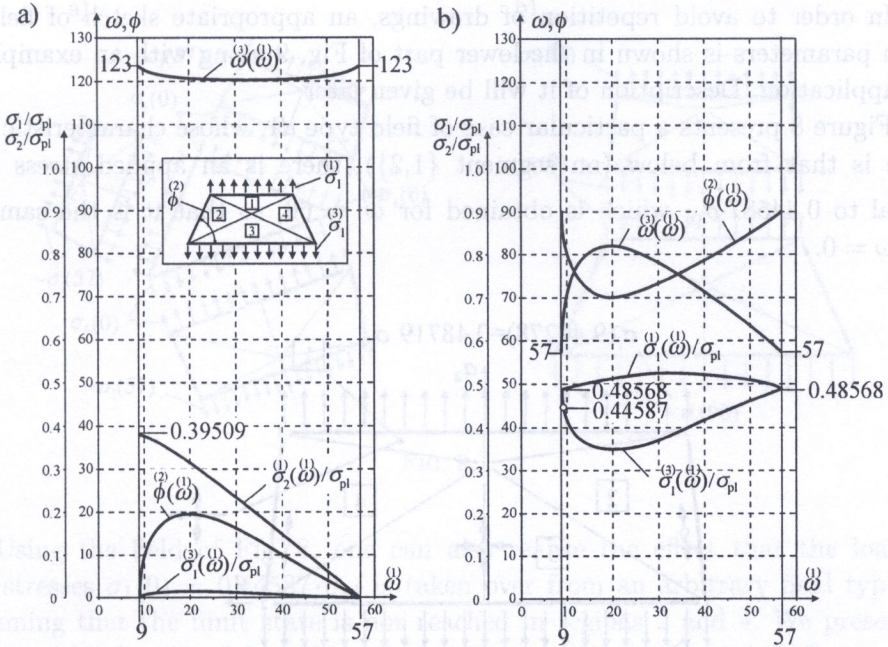


FIG. 7. Selected parameter functions and boundary stresses in limit field type  $d1$   
 a) for  $\phi = 0^\circ$ ; b) for  $\phi = 90^\circ$ .

Although the limit field having line system structure type  $d1$  can not be constructed for the angles from the interval of  $\phi \in (20^\circ, 70^\circ)$ , the boundary conditions, pertaining to such a range of angles, are very often met in practice. For example, we obtain a value of angle  $\phi$  from this interval if we take  $\omega = 90$  in region 3, in other words, when assuming pure shear in this region. In this case, when we take  $\omega = 57$  in region 2 we obtain such values of angle  $\phi$  that the yield condition is exceeded in region 1.

The way out of this difficulty is not to attempt to reach the limit state in regions 2 and 4, but, instead, assume there the stress multiplier equal to  $x = 0.91803923$ , in effect of what one can obtain  $\sigma_1^{(2)} = \sigma_1(0) = 0.44587 \cdot \sigma_{pl}$  in this region. Due to of this concession, one gains the possibility of making use of the state  $\omega^{(1)} = 0$  in region 1, and the freedom of creating branching of the strips, similarly as it was possible in the field type  $z0$ . Obviously, the stress discontinuity line separating regions 2 and 1 will be perpendicular to the direction of principal stress  $\sigma_1$ , similarly to the case of field  $d1$  created for the Huber–Mises or Tresca conditions.

In order to avoid repetition of drawings, an appropriate sketch of field of such parameters is shown in the lower part of Fig. 9 along with an example of its application. Description of it will be given later.

Figure 8 presents a particular case of field type  $d1$ , whose characteristic feature is that from below (on segment  $\{1,2\}$ ), there is an applied stress load equal to  $0.44587 \cdot \sigma_{pl}$  which is obtained for  $\omega = 66$ , so that it is the same as for  $\omega = 0$ .

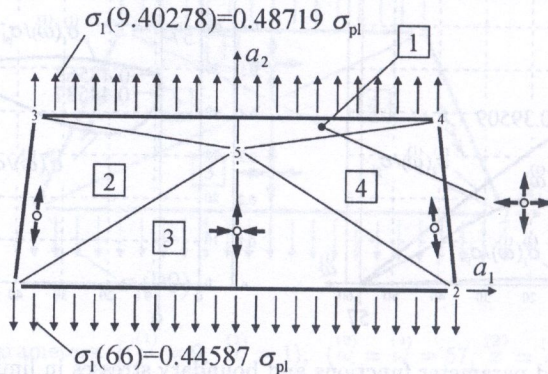


FIG. 8. Field parameters:  $\{(\omega^{(1)} = 9.40278, x^{(1)} = 1.0031), (\omega^{(2)} = 57, x^{(2)} = 1), (\omega^{(3)} = 66, x^{(3)} = 1), (\omega^{(4)} = 57, x^{(4)} = 1)\}$ .

In region 2 we have, as in the previous case,  $\sigma_1(57) = 0.48568 \cdot \sigma_{pl}$ . With these assumptions, one obtains two roots of parameters  $\omega = 9.40278$  and  $\omega = 47.25827$  in region 1. The stresses  $\sigma_1$  for the root  $\omega = 9.40278$  are equal to  $0.48719 \cdot \sigma_{pl}$ , and are not significantly greater than  $\sigma_1(57) = 0.48568 \cdot \sigma_{pl}$  in the tensioned strip. The difference appears only at the third decimal position. It seems that, in practical conditions, we can well tolerate such an insignificant exceeding of the yield condition ( $x = 1.0031$ ) in the strip built above the segment  $\{3,4\}$ , the more so that there are not any other solutions to limit fields type  $d1$  in which stresses equal to  $\sigma_1(0)$  and (approximately)  $\sigma_1(57)$  are applied from below and from above, respectively. Then, we can make use of this field in the same way as if the stress applied from above was actually equal to  $\sigma_1(57)$ .

Owing to this property, the previously mentioned solution appears to be one of the most important ones for the Oyane condition. It makes it possible, among other things, to combine three such fields to construct, for this condition, an equivalent of the field type  $z0$ , as shown in Fig. 9a.

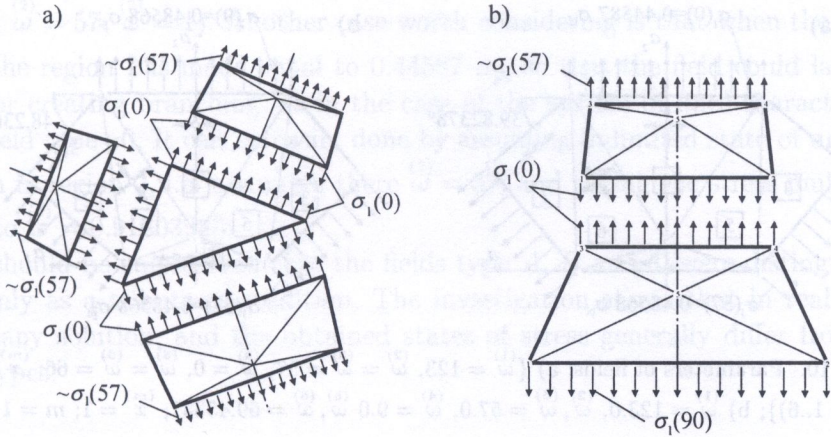


FIG. 9.

Using the field of Fig. 8, one can also realise the effect that the load of the stresses  $\sigma_1(0) = 0.44587 \cdot \sigma_{pl}$  is taken over from an arbitrary field type *d1* assuming that the limit state is not reached in regions 2 and 4. We presented an example of such a field in Fig. 6 assuming pure shear in region 3. Connecting such fields in the way shown in Fig. 9b, we obtain a complex field, which can take over practically arbitrary loads of admissible values from below, and which can be balanced from above by limit reactions of the tensioned (or compressed) strip, which are equal to  $0.48719 \cdot \sigma_{pl}$ . As it can be seen, in order to achieve such a freedom of choice of the load value at the lower boundary, one needs as many as two component fields type *d1*. With the Huber-Mises or Tresca conditions, one such field was sufficient.

For the second root  $\omega^{(1)} = 47.25827$ , on the upper boundary of the field (on segment {3,4}), we obtain stresses of values  $\sigma_1^{(1)} = 0.51526 \cdot \sigma_{pl}$ , which exceed the limit stress, equal to  $\sigma_1(57)$  in the tension strip. The importance of this solution seems to be marginal.

Figure 10 presents two new systems of stress discontinuity lines obtained for the Oyane condition, whose structure of line system is different from that assumed in fields type *d1*.

The first one (Fig. 10a) was found in the result of seeking for such a limit field in the connection region between two tension strips, in which the load is received from region 4 with  $\omega^{(4)} = 0$ .

In view of the fact that the state adjacent to  $\omega^{(4)} = 0$  can only be  $\omega = 66$ , one must design intermediate regions 5 and 6, where  $\omega^{(5)} = \omega^{(6)} = 66$ . Only from these regions we can draw the strips in which we have  $\omega^{(2)} = 57$ . In region 1 we have  $\omega^{(1)} = 123$ .

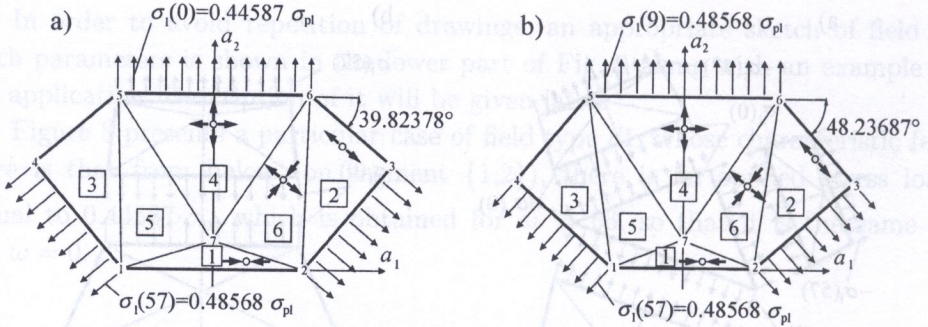


FIG. 10. Parameters of fields: a)  $\{\omega^{(1)} = 123, \omega^{(2)} = \omega^{(3)} = 57, \omega^{(4)} = 0, \omega^{(5)} = \omega^{(6)} = 66; x = 1; m = 1.6\}$ ; b)  $\{\omega^{(1)} = 123.0, \omega^{(2)} = \omega^{(3)} = 57.0, \omega^{(4)} = 9.0, \omega^{(5)} = \omega^{(6)} = 69.45357; x = 1; m = 1.6\}$ .

The presented solution is rather characteristic for the Oyane condition. Unfortunately, it can be obtained only for particular boundary conditions.

Figure 10b depicts another, new limit field, in which all stresses on loaded boundaries are equal to  $\sigma_1(57) = 0.48568 \cdot \sigma_{pl}$ . The case is then different from that of fields *d1* in Fig. 9a, where this equality was fulfilled only approximately. Therefore, the field of Fig. 10b fulfils the same boundary conditions as a field type *z0*. However, the field was obtained here only for particular values of angles between the axes of the converging strips.

### 2.3. Remarks on characteristic fields around nodes

One can not find any significant distinctness in the fields type *A* and *B* constructed for the Oyane condition that arise around concave and convex vertices ([1], Fig. 11 a, b). The only characteristic feature is the reduced number of solutions, which is a natural consequence of elimination of the roots related to  $\omega = 0$  – that exist for the Huber-Mises and Tresca conditions.

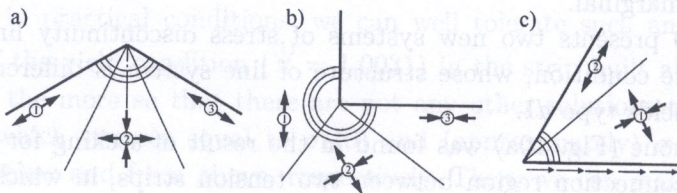


FIG. 11.

The field type *C* ([1], Fig. 11c) is loaded on one boundary with shear stress. It was assumed in the example shown in the figure that the stress value is equal to  $0.2 \cdot \sigma_{pl}$  and that the stresses in regions 1 and 2 take limit states ( $\omega = 113.19363$ ,

$x = 1$ ;  $\omega = 57$ ,  $x = 1$ ). Another case worth considering is that when the stress  $\sigma_1$  in the region 2 is made equal to  $0.44587 \cdot \sigma_{pl}$  so that the field could later be used for creating branching, as in the case of the system of lines characteristic for a field type  $z0$ . It can be easily done by assuming unlimited state of uniaxial tension in region 2, i.e. assuming there  $\omega = 57$ , and taking the stress multiplier equal to  $x = 0.91803923$ .

It should be emphasised that the fields type *A*, *B* and *C* were distinguished here only as a tribute to tradition. The investigation shows that in reality we find many solution, and the obtained states of stress generally differ from the prototypes.

### 3. CONCLUDING REMARKS

The fact that for  $f_v > 0$  and Oyane-type medium with plane stress, the values of stresses  $\sigma_1(0) = \sigma_2(0)$  are lower than limit stresses in the tension strips (here  $\sigma_1(57)$ ), makes it impossible to use the systems of stress discontinuity lines constructed with the Huber–Mises or Tresca conditions to the analyses of the Oyane limit fields. These systems are different moreover, this conclusion applies to a vast majority of frequently encountered complex systems. Then, in all these cases, in order to find the field for the Oyane condition, one should either modify the known systems, or look for new ones.

In the other case this would mean the necessity of solving the boundary problems, encountered there, from the very beginning, namely from the phase when even the system of lines is not known. Fortunately, we do not need to foresee these systems ([9]), but the task is not so simple, anyway, even if one makes use of the existing algorithms. Despite application of a methodical approach, significant difficulties appear in controlling the abundance of the obtained solutions. However, if one only needs to find the field parameters, and the structure of line system is already known, no significant difficulties are expected.

The question then arises is it possible to avoid solving such difficult problems for the Oyane condition, at least in applications, and instead to use there the already known line systems found for the Huber–Mises condition?

The arguments for a positive answer to this question follow from the above-presented numerical values. For example, for the porosity ratio  $f_v \approx 0.3$  assumed in this study, whose value is relatively high, the stresses in the tension strips of the field type  $z0$  shown in Fig. 5 can be as high as over 90% of their limit values. Such a difference lies within the error interval of the SADSf method. The limit curve would be, in this case, the ellipse inscribed into the Oyane curve, as shown in Fig. 2a. The contours of elements, obtained upon assuming such a limit curve,

would lie on the safe side. Obviously, the systems of lines associated with it would be characteristic for the Huber–Mises, not Oyane condition.

The greatest collection of such systems, constructed for the Huber–Mises condition with diverse boundary conditions, is contained in the software library, which constitutes an integral part of the work [3].

#### REFERENCES

1. W. SZCZEPIŃSKI *Plastic design of machine parts* [in Polish], PWN, Warszawa, 1968.
2. M. OYANE, S. SHIMA, Y. KONO, *Theory of plasticity for porous metals*, Bull. JSME, **16**, 1254–1262, 1973.
3. I. MARKIEWICZ, *Numerical determination of statically admissible link systems of stress discontinuity lines in limit the Huber–Mises's fields* [in Polish], PhD thesis, Warsaw University of Technology, 1996.
4. J. MIELNICZUK, *Plasticity of porous materials. Theory and the limit load capacity*, Poznań University of Technology, 2000.
5. J. MIELNICZUK, R. MOSTOWSKI, *Designing porous structural elements by the use of the limit analysis method* [in Polish], WSP Zielona Góra 2000.
6. W. SZCZEPIŃSKI, J. SZLAGOWSKI, *Plastic design of complex shape structures*, Ellis Horwood & PWN, Warszawa – Chichester 1990.
7. W. BODASZEWSKI, A. BUCZYŃSKI, *Domain existence limit stress discontinuity system in Oyane porous media*, 34-th Solid Mechanics Conference, SolMec 2002.
8. W. BODASZEWSKI, *Stress discontinuity line structures in yield zones satisfying the the Huber–Mises condition* [in Polish], Engng. Trans., part 1 **36**, 1, 29–54, 1988; part 2 **37**, 3, 415–442, 1989.
9. W. BODASZEWSKI, *Algorithms of the method of statically admissible discontinuous stress fields (SADSF)*, Engng. Trans., (Part I – 3/2004, remaining 3 parts – in print).
10. W. BODASZEWSKI, *The software package KNPN for approximated shaping of complex plastic structures*, VIII-th Symposium on Stability of Structures, Łódź University of Technology, 25–30, 1997.
11. Internet website [www.sadsf.net](http://www.sadsf.net)

Received December 1, 2004.